processes

MDPI

Article

Comparative Study of Binder Stability for Aqueous Lithium-Ion and Solid-Boosted Flow Batteries

Silver Sepp [1,*], **Maarja Paalo** [1] and **Pekka Peljo** [2,3]

[1] Institute of Chemistry, University of Tartu, Ravila 14a, 50411 Tartu, Estonia; maarja.paalo@ut.ee
[2] Department of Mechanical and Materials Engineering, University of Turku, 20014 Turku, Finland; pekka.peljo@utu.fi
[3] Department of Chemistry and Materials Science, Aalto University, P.O. Box 16100 Aalto, 00076 Espoo, Finland
* Correspondence: silver.sepp@ut.ee

Abstract

The replacement of polyvinylidene fluoride (PVDF) with environmentally friendly binders offers potential advantages in the development of aqueous lithium-ion batteries (ALIBs) and flow batteries (FBs) incorporating solid charge carriers (so-called solid boosters). This study investigates the electrochemical stability of ethyl cellulose and cross-linked gluten as substitutes for PVDF in $LiMn_2O_4$ (LMO) cathodes for aqueous Li-ion battery electrodes and solid boosters for FBs. The millimetre-scaled solid booster beads must be easily produced on a large scale, and at the same time, their charging and discharging must be reversible over long durations under electrolyte tank conditions. The binders were tested under standardized conditions for discharge capacity and cycling stability. Our results demonstrate that ethyl cellulose and cross-linked gluten can rival the electrochemical stability of PVDF, maintaining initial discharge capacities near 100 mAh g^{-1} at 0.2 C for LMO cathodes and exhibiting reasonable capacity retention over hundreds of cycles. This work supports the feasibility of sustainable electrode processing, provides promising directions for scalable, eco-friendly electrode fabrication methods, and highlights promising binder candidates for use in aqueous energy storage systems.

Keywords: lithium-ion battery; eco-friendly binder; flow battery

Academic Editors: An-Ya Lo, Yu-Cheng Chang and Chelliah Koventhan

Received: 15 September 2025
Revised: 9 October 2025
Accepted: 15 October 2025
Published: 18 October 2025

Citation: Sepp, S.; Paalo, M.; Peljo, P. Comparative Study of Binder Stability for Aqueous Lithium-Ion and Solid-Boosted Flow Batteries. *Processes* **2025**, *13*, 3338. https://doi.org/10.3390/pr13103338

1. Introduction

Global decarbonization is accelerating demand for safe, scalable, and sustainable electrochemical storage. Aqueous lithium-ion batteries (ALIBs) and flow batteries (FBs) incorporating solid boosters (Figure 1) are attractive for stationary applications, but performance and durability hinge on the binder—whether it glues active material, carbon, and current collector in electrodes or binds millimetre-scale particles in boosters [1–6].

In traditional lithium-ion batteries, polyvinylidene fluoride (PVDF) is the standard binder owing to its chemical stability, electrochemical inertness, and mechanical robustness. However, its reliance on N-methyl-2-pyrrolidone (NMP)—a toxic, high-boiling solvent—and its fluorinated (PFAS) nature pose environmental and regulatory challenges, especially for large-scale manufacturing and end-of-life handling. These concerns are particularly acute for solid-booster implementations, where high-volume binder processing magnifies environmental impact. Reflecting global moves to phase out PFAS, several manufacturers have already adopted PFAS-free, water-processable binders that eliminate PVDF/NMP and improve safety [4,7–14].

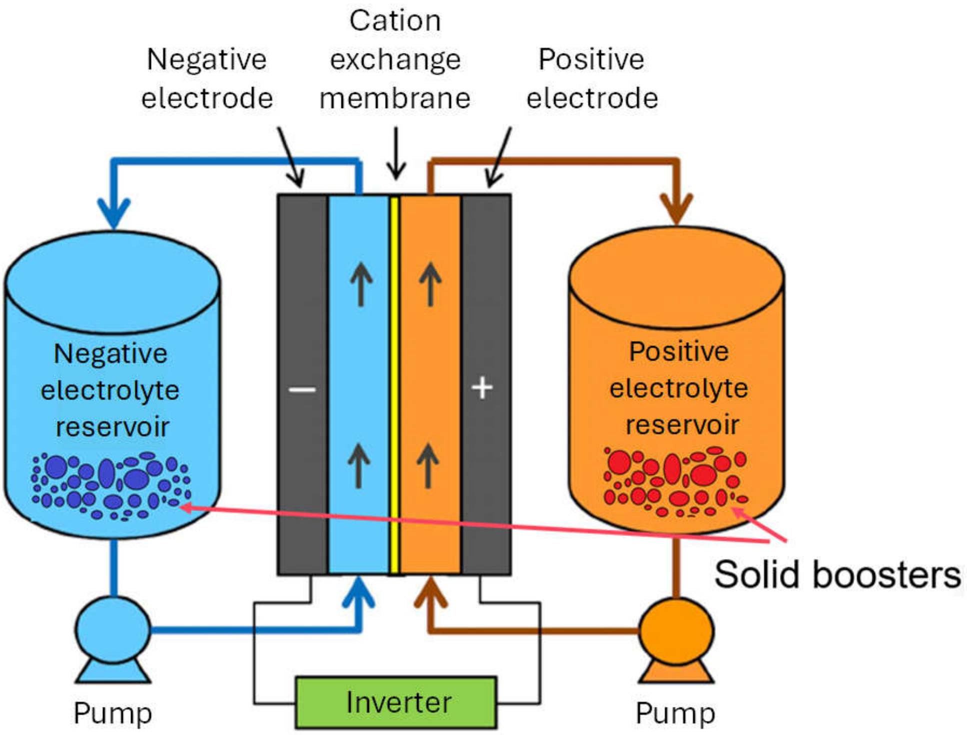

Figure 1. Schematic of a flow battery with solid boosters.

Accordingly, there is strong momentum toward water/alcohol-processable and bio-derived binders that avoid NMP and fluorinated polymers [8–10,15,16]. Ethyl cellulose (EC) is processable in benign alcohols and has shown promising adhesion and electrochemical compatibility in aqueous systems [9,10,16]. Protein-based binders such as wheat gluten become water-insoluble after thermal cross-linking (e.g., via disulfide formation), yielding flexible networks suitable for aqueous processing [17,18]. While PVDF remains the inertness benchmark, its hydrophobic and electrically insulating character can impair wetting and percolation at elevated loadings, limiting capacity and rate performance [11,19–23].

Within these systems, $LiMn_2O_4$ (LMO) is widely employed because of its thermal stability, low cost, and high-voltage plateau; its practical capacity (~100–120 mAh g^{-1}) is somewhat below its theoretical value (~148 mAh g^{-1}) [2,3]. Recent reviews highlight key factors governing natural-polymer binder performance—adhesion, swelling behaviour, electrochemical stability, and interactions with active materials—which we summarize for PVDF, EC, and cross-linked gluten in Table 1.

Previous studies have shown that binder degradation can severely impact long-term cycling stability, capacity retention, and coulombic efficiency of batteries [4–6,24,25]. A notable gap in the literature is a head-to-head evaluation of multiple green binders under identical aqueous protocols with explicit consideration of solid-booster constraints. Solid boosters—binder-containing, millimetre-scale beads that remain in electrolyte tanks—must endure continuous immersion, abrasion, and long-duration cycling without swelling or disintegration, imposing stricter demands on water-stability, cohesion, and interfacial transport [1].

This work aims to address that gap by comparing the electrochemical stability and performance of EC and thermally cross-linked gluten against PVDF using $LiMn_2O_4$ (LMO) as the cathode active material, selected for its compatibility with aqueous electrolytes and well-defined Mn^{3+}/Mn^{4+} redox couple [2,3]. Our central hypothesis is that EC and cross-linked gluten can match or exceed PVDF in electrochemical stability for ALIB electrodes and solid boosters while enabling PFAS-free, sustainable processing [13,26]. The goal is to identify viable alternatives that combine environmental sustainability with mechanical and electrochemical reliability for both ALIBs and solid-boosted flow batteries.

We position this study as a true side-by-side benchmark of EC and cross-linked gluten versus PVDF under identical aqueous conditions, with specific novelty in the context of solid-booster operation (continuous immersion and abrasion resistance). We situate the results within recent advances in aqueous electrode manufacturing and binder design [4–6,8–10,15,16,18,19,21,27,28], emphasizing how binder chemistry and loading govern electronic/ionic percolation, wetting, swelling, and mechanical cohesion in water. The analysis clarifies practical trade-offs among initial capacity, rate capability, and long-term stability for PVDF, EC, and gluten, guiding sustainable binder selection for aqueous lithium-ion systems and solid-boosted flow batteries [12,14,22,23,26,29].

Table 1. Key properties of PVDF, ethyl cellulose, and cross-linked gluten binders in aqueous battery electrodes (ALIBs/RFBs).

Property	PVDF (Baseline)	Ethyl Cellulose (EC)	Cross-Linked Gluten
Binder Type	Synthetic fluoropolymer (non-renewable)	Modified natural polymer (cellulose ether derivative)	Natural protein polymer (wheat gluten), thermally cross-linked
Solvent Requirement	NMP (toxic, high boiling point) [11]	Ethanol or isopropanol (benign, low toxicity) [9,10]	Water-based slurry (green process); heat curing required [17,18]
Mechanical Properties	Highly flexible and tough; excellent adhesion to particles [6,21]	Good adhesion; moderate flexibility (sufficient for cohesion) [4]	Flexible, rubbery network after crosslinking; strong cohesion [17,18]
Water Stability	Hydrophobic and chemically inert in water (no swelling or dissolution) [11]	Water-insoluble; minimal swelling (maintainsstructure) [16]	Water-insoluble after crosslink; slight swelling possible but no dissolution [17]
Environmental Impact	Requires toxic solvent; not biodegradable; fluorinated (hazardous disposal) [4,7]	Renewable source; solvent is low-toxic and recyclable; biodegradable over time; no fluorine [9,10]	Renewable and biodegradable; no organic solvent needed; no fluorine—safe disposal [17]
Processing Complexity	Established slurry casting with NMP, but needs strict safety controls and drying infrastructure [11]	Simple slurry mixing in alcohol; fast drying; flammable solvent handling needed (standard lab safety) [15]	Easiest: aqueous slurry in ambient conditions; requires thermal cross-link step [17]
Electrochemical Stability	Electrochemically inert; stable in wide potential window (up to ~4.2 V vs. Li^+ in organics) [19]	Inert within aqueous voltage window; no redox-active groups; stable in neutral pH [8,16]	Largely inert after curing; no significant degradation observed within water stability window (mild conditions) [28]

2. Materials and Methods

2.1. Materials

$LiMn_2O_4$ (LMO, high-purity, commercial grade) was used as the active cathode material; this spinel-type lithium manganese oxide is widely employed in aqueous battery systems due to its good thermal stability, abundant raw materials, and relatively high potential plateau (~4 V vs. Li/Li^+) [3]. Carbon black (Super P, >99% C, Timcal, Bodio, Switzerland) served as the conductive additive. The tested binders included polyvinylidene fluoride (PVDF, Solef 5130, Arkema, Colombes, France), ethyl cellulose (EC, Sigma-Aldrich, St. Louis, MI, USA, viscosity ~10 mPa·s, 48% ethoxyl substitution, Darmstadt, Germany), and wheat gluten (food-grade, Sigma-Aldrich), which was cross-linked in situ by heat treatment. Water (deionized, Milli-Q system, Merck Millipore, Darmstadt, Germany), ethanol (99.5%, Sigma-Aldrich) and isopropanol (IPA, 99.7%, Sigma-Aldrich) were used as solvents.

In all electrode formulations, the active material fraction was fixed at 80 wt%. Binder and conductive additive contents were varied between 5 and 10 wt% binder and 10–15 wt% Super P (making a total of 20% binder + carbon). For example, a "5% binder" electrode contained 5 wt% binder + 15 wt% Super P, whereas a "10% binder" electrode contained 10 wt% binder + 10 wt% Super P (with LMO 80 wt% in both cases). All experiments were conducted in ambient laboratory conditions. Binder contents of 5% and 10% chosen to represent common industrial bounds. The electrolyte for all tests was an aqueous 1 M $LiNO_3$ solution (99.999%, Thermo Scientific, Waltham, MA, USA).

2.2. Electrode Preparation and Characterization

Binder-containing slurries were prepared using appropriate solvents: NMP was used for PVDF (as per standard practice for PVDF binders), ethanol for ethyl cellulose, and deionized water for gluten. The slurry preparation for the bio-based binders followed protocols adapted from prior work on water processable electrodes [30,31]. The LMO active powder and Super P conductive carbon were weighed into a vial (100 mg total solids). For EC or gluten formulations, the binder powder was added, followed by 1 mL of the corresponding solvent (ethanol for EC, water for gluten), and the slurry was mixed to homogeneity. For PVDF, the polymer was first dissolved in NMP (1 mL) with 4 h stirring at room temperature and left overnight. The resulting PVDF/NMP solution was then added to the pre-weighed LMO–Super P mixture and stirred to obtain a uniform slurry. For PVDF and ethyl cellulose, the slurries were drop-cast onto the current collector (glassy carbon disc or carbon–polymer composite substrate) and dried at ambient temperature to evaporate the solvent. Gluten-based electrodes required an additional curing step: after drying the aqueous gluten slurry coating, the electrode was heated at 150 °C for 1 h to induce thermal cross-linking of the gluten. This thermal treatment causes gluten proteins to form intermolecular bonds (e.g., disulfide bridges), yielding a water-insoluble, rubbery network that improves the binder's mechanical integrity and water resistance [17]. No additional chemical cross-linkers were used. Active-material loading was 1.6 mg cm^{-2} (2.0 mg cm^{-2} total, 80 wt% LMO).

Analyses and imaging were carried out using a Zeiss EVO MA15 (Zeiss, Jena, Germany) scanning electron microscope equipped with an Oxford Instruments X-MAX energy-dispersive spectroscopy (EDS) detector (Oxford Instruments, Abingdon, UK). The acquired spectra were processed and quantified using Aztec 5.0 software (Oxford Instruments, Abingdon, UK). All measurements were conducted in variable-pressure mode to minimize surface charging of uncoated or poorly conductive samples. The accelerating voltage was set to 20 keV.

2.3. Electrochemical Measurements

Electrochemical stability was evaluated using cyclic voltammetry (CV) and galvanostatic charge–discharge cycling. A three-electrode cell (Teflon body, custom-made in-house) was assembled for testing, with Ag/AgCl (3 M KCl) as the reference electrode, a platinum wire as the counter electrode, and the prepared LMO-based electrode as the working electrode and 1 M $LiNO_3$ as the electrolyte. All measurements were conducted at room temperature (~22 °C). CV measurements were carried out using a Gamry Reference 600+ potentiostat (Gamry Instruments, Warminster, PA, USA), typically scanning between 0.8 and 1.2 V vs. Ag/AgCl (spanning the Mn^{3+}/Mn^{4+} redox window of LMO in aqueous media) at 2 mV s^{-1}. These scans were used to assess the electrochemical inactivity of the binder itself and to verify that the characteristic LMO redox peaks (~0.9–1.0 V vs. Ag/AgCl) appeared with each binder, indicating similar electrochemical reactions in all cases. For galvanostatic cycling, electrodes were tested in two modes: (i) a rate capability test where the discharge current was sequentially increased to evaluate performance under higher C-rates, and (ii) a long-term cycling test at a fixed current (1 C rate) to assess capacity retention over hundreds of cycles. In the rate test, a LANHE battery tester (Model G340A, Wuhan LAND Electronic Co., Ltd., Wuhan, China) was used to cycle the electrodes for 6 cycles at each of several rates (0.2 C, 0.5 C, 1 C, 2 C, 5 C), and then finally return to 0.2 C, each segment lasting 6 cycles (total 36 cycles per test). The charge/discharge cutoff was set to a fixed capacity limit or voltage range (equivalent to ~1.0–1.2 V vs. Ag/AgCl for full charge). For long-term durability, separate electrodes were continuously cycled at 1 C (charge and discharge each 1 h) for 500 cycles or until failure, using the same three-electrode configuration (with excess lithium nitrate electrolyte to avoid exhaustion of Li^+). Specific capacities (mAh g^{-1}) were calculated based on the mass of LMO active material and are reported for the discharge (lithium extraction from LMO) half-cycle.

3. Results

3.1. Cyclic Voltammetry of Electrodes

All three binder types yielded qualitatively similar cyclic voltammograms for the LMO cathodes in the aqueous electrolyte, indicating that the choice of binder did not significantly alter the fundamental electrochemical reactions of the active material. Characteristic redox peaks for the Mn^{3+}/Mn^{4+} couple of LMO were observed around 0.9–1.0 V vs. Ag/AgCl in all cases (Figure 2). There were no extra peaks or currents in the CVs that would indicate binder decomposition or parasitic side reactions within the water stability window (~0–1.23 V vs. Ag/AgCl). This suggests that PVDF, ethyl cellulose, and cross-linked gluten are all sufficiently inert (after curing) under the mild potentials experienced by the LMO cathode in aqueous media. One subtle difference noted was a slightly higher internal resistance (larger peak separation) for the electrodes with 10% PVDF, consistent with its higher content of non-conductive binder. The CV window (≈0.8–1.2 V vs. Ag/AgCl) targets the operative range; potential parasitic processes outside this window will be probed in expanded-window follow-ups. Overall, the CV results confirmed that the alternative binders do not introduce new redox activity and that any performance differences in cycling are likely due to physical/mechanical effects rather than electrochemical side reactions.

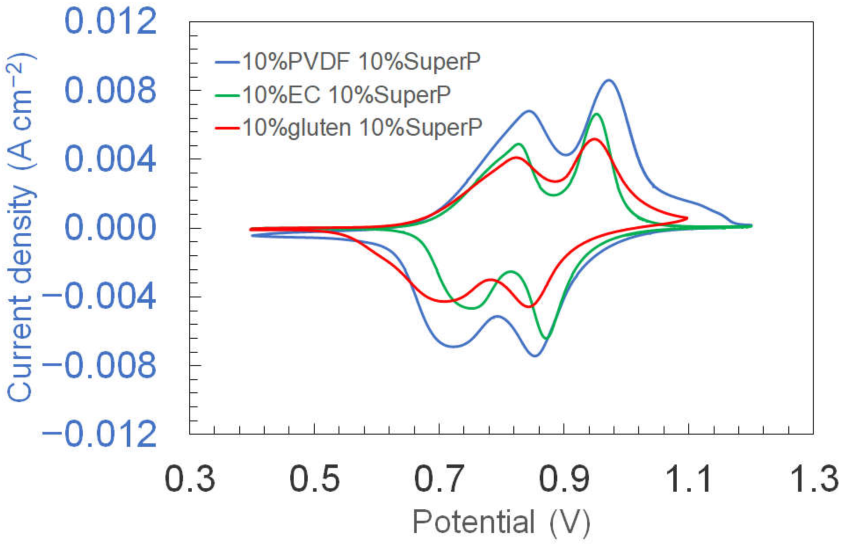

Figure 2. Cyclic voltammograms of LMO cathodes with PVDF, ethyl cellulose (EC), and cross-linked gluten binders (all 10 wt% content) in 1 M $LiNO_3$ at a scan rate of 2 mV/s.

3.2. Rate Performance and Initial Capacity Comparison

The initial specific capacities and rate performance of LMO cathodes were strongly influenced by both the binder type and binder content. Figure 3 presents the discharge capacity versus cycle number for each binder formulation during the multi-rate test. In this test, all electrodes were initially cycled at 0.2 C (cycles 1–6), then the rate was progressively increased to 0.5 C, 1 C, 2 C, 5 C in steps (each rate for 6 cycles), and finally returned to 0.2 C (last 6 cycles). This protocol allows evaluation of how capacity fades with increasing C-rate and how well it recovers when returning to a low rate. Several trends are evident in Figure 3. While CV measurements (Figure 2) confirmed the electrochemical inertness of all binders, the much lower capacity of 10% PVDF in Figure 3 arises from its insulating nature, excessive loading, and reduced electrode wettability. This phenomenon is consistent with literature reports [11,20]. At a fixed scan rate, CV confirms the presence and reversibility of the Mn^{3+}/Mn^{4+} couple in LMO but does not quantify the practical discharge capacity. In galvanostatic cycling, the deliverable capacity is limited by transport and ohmic/polarization losses that depend on the electrode microstructure and binder content.

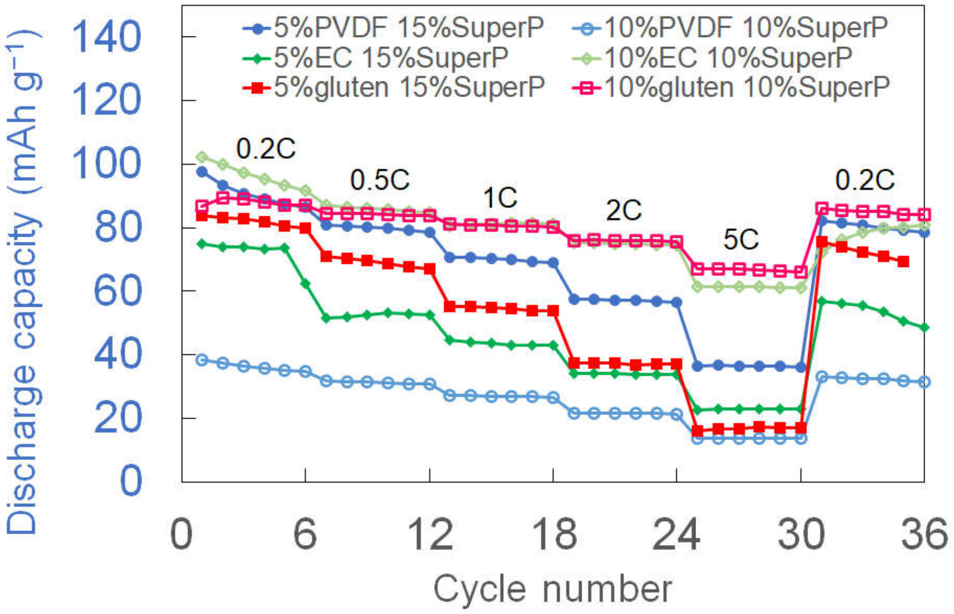

Figure 3. Discharge capacity vs. cycle number for LMO cathodes with PVDF, ethyl cellulose (EC), or gluten binders at 5 wt% and 10 wt% content (with Super P adjusted to 20 wt% total).

PVDF is widely regarded for its chemical stability and strong binding ability; however, this study shows that excessive PVDF content (10%) severely compromises electrochemical performance. The 10% PVDF sample exhibits markedly low initial specific capacity (~38 mAh g^{-1}), which remains suppressed throughout the cycling test. In contrast, the 5% PVDF sample delivers a much higher initial capacity (~98 mAh g^{-1}) and maintains it with minimal degradation. The poor performance at 10% can be attributed to over-insulation of active material particles, leading to poor electronic conductivity and reduced ionic accessibility. Excess PVDF may also form dense films that block electrolyte infiltration and increase electrode resistance [11,20]. By contrast, the 5% PVDF electrode, with more conductive carbon available, maintained good electronic conductivity and thus much better capacity at high rates. These results highlight that while PVDF is chemically stable, its non-conductive nature means the loading must be optimized to avoid degrading the electrode's power capability.

Ethyl cellulose demonstrates promising results, particularly at 10% content, where it achieves the highest initial capacity among all samples (>100 mAh g^{-1}). This suggests that ethyl cellulose forms a favourable network structure that facilitates ion transport and maintains mechanical cohesion. Unlike PVDF, a higher content of ethyl cellulose does not seem to impede performance significantly. However, both 5% and 10% ethyl cellulose samples exhibit a gradual capacity decline, possibly due to partial solubility or mechanical fatigue of the organic binder over extended cycles. This somewhat counterintuitive result (the higher binder content yielding better high-rate retention) could be due to the 5% EC electrode having insufficient binder to maintain conductive network integrity under stress. With only 5% EC, the electrode may be more prone to micro-cracking or particle detachment as the current increases and slight volume changes or mechanical stresses accumulate, whereas 10% EC provides a more robust network that holds the composite together at high rates. Another factor is that the 5% EC electrode had 15% carbon which boosts electronic conductivity, but if the binder is too low, the carbon and active particles might not be held in close contact during rapid cycling.

Gluten-based electrodes show clear performance advantages at 10% binder content. The 10% gluten sample delivers higher initial capacity (~89 mAh g^{-1}) and significantly greater capacity retention under cycling and increasing C-rates compared to the 5% sample (~84 mAh g^{-1}). These results indicate that gluten requires a sufficiently high content to form a robust, cross-linked matrix that maintains mechanical cohesion and ensures uniform current distribution. The 5% gluten formulation, while still functional, suffers from faster capacity fading and weaker retention, likely due to insufficient binder coverage or less effective particle binding. These findings underscore that 10% gluten content is optimal within the tested range, and that binder-specific tuning is critical for bio-derived systems.

A critical component of this study involved assessing capacity retention as C-rates increased, mimicking high-power demand conditions. Among the binder types, the performance trends varied depending on the formulation. The reduced performance of 10% PVDF can be attributed to several mechanisms: (1) increased binder content dilutes active material per unit mass, (2) dense fluoropolymer films impede lithium-ion transport and reduce wettability, and (3) PVDF's non-conductive nature exacerbates internal resistance buildup. In contrast, the performance of gluten and ethyl cellulose at 10% indicates better ionic and mechanical integration without excessive impedance. For ethyl cellulose and gluten, the 10% binder content generally resulted in more stable capacities, especially at moderate and high C-rates. These results suggest that bio-based binders may require higher content to ensure cohesion and continuous conductive networks under fast cycling conditions.

Overall, these findings underscore the importance of binder-specific optimization: while lower PVDF content enhances capacity retention, higher gluten or ethyl cellulose content may improve performance, particularly under high-rate cycling. Across repeats ($n \approx 3$), initial discharge capacity varied by ±5%. Future work should examine binder–additive synergies, cross-linking behaviour, and long-term effects of formulation on ionic/electronic transport pathways.

3.3. Long-Term Cycling Stability

While rate performance tests the immediate capacity under stress, long-term cycling reveals how each binder sustains the electrode over many charge–discharge cycles. Figure 4 shows the discharge capacity retention over 500 galvanostatic cycles at 1 C for LMO electrodes with 10% binder (PVDF, EC, or gluten; all with 10% Super P). These conditions accelerate any binder degradation or electrode deterioration, as 1 C cycling for hundreds of cycles in aqueous media is a stringent test (notably, LMO itself can suffer capacity fade from Mn dissolution in aqueous electrolytes over long term).

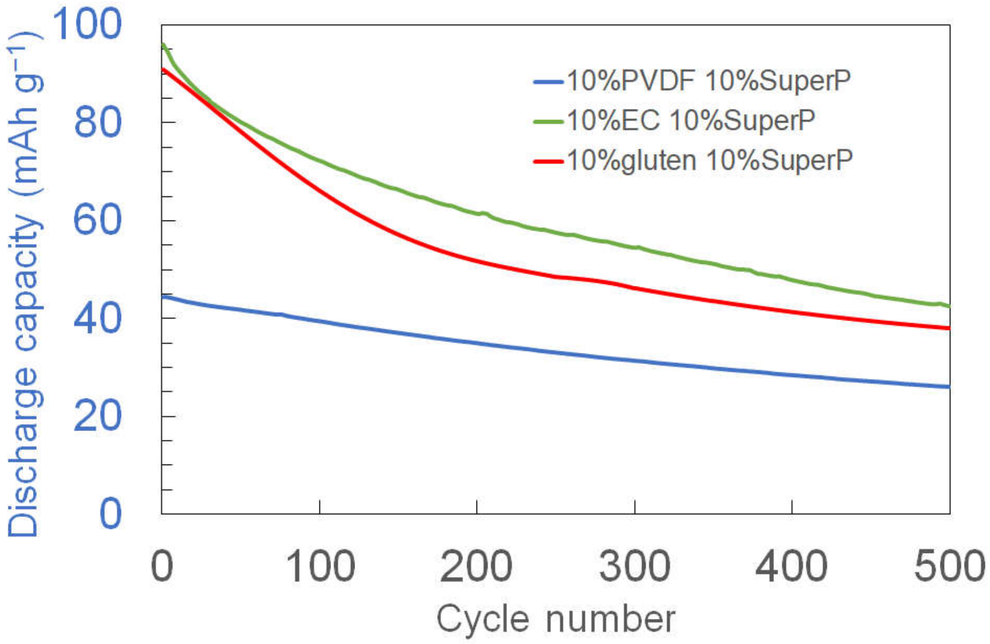

Figure 4. Long-term cycling performance of LMO electrodes at 1 C in 1 M $LiNO_3$ with 10 wt% binder (PVDF, ethyl cellulose (EC), or cross-linked gluten) and 10 wt% Super P.

As seen in Figure 4, the PVDF-based electrode displays a relatively stable but low capacity over 500 cycles. It begins around 40 mAh g^{-1} at cycle 1 (consistent with the earlier observation of suppressed capacity for 10% PVDF at 1 C) and very gradually fades to about 26 mAh g^{-1} by cycle 500. The capacity decay is mild and linear, indicating that PVDF itself remains chemically and mechanically intact; the loss is likely due to LMO's known failure modes (e.g., Mn leaching, or electrolyte/interface changes) rather than the binder. This aligns with PVDF's reputation for excellent inertness and mechanical resilience—it imposes performance limitations (low initial capacity) but does not dramatically break down over time.

The ethyl cellulose 10% electrode starts with a much higher discharge capacity (around 100 mAh g^{-1} at cycle 1, thanks to EC's low initial impedance). However, it exhibits a more pronounced fade over the 500 cycles. By 100 cycles, the EC electrode's capacity drops to ~80 mAh g^{-1}; by 300 cycles, it is around ~60 mAh g^{-1}; and by the end of 500 cycles, it approaches ~50 mAh g^{-1}. Despite this decline, it still slightly surpasses the PVDF electrode's capacity at the end of the test. The more significant fading in the EC-bound electrode could stem from a gradual deterioration of the binder's binding ability—for instance, slow swelling, mechanical fatigue (micro-cracks forming under repeated strain), or minor dissolution of any un-crosslinked polymer chains. Additionally, because the EC electrode started at a higher capacity, it may be more susceptible to LMO's intrinsic issues (like Mn dissolution) which are exacerbated at higher utilization levels. Nonetheless, the EC binder maintained the electrode cohesion well enough that catastrophic failure was avoided; the capacity decay flattened out in later cycles, suggesting that after an initial drop, the system stabilized. This result is promising because even without any special additives or optimizations, the EC binder allowed for a 2–3 times higher capacity than PVDF in early cycles and still comparable capacity after 500 cycles. Minor improvements (such as cross-linking EC or blending with a co-binder) could further improve its stability.

The cross-linked gluten binder showed a mixed outcome. Initially, the 10% gluten electrode matched the ethyl cellulose's high capacity (~90 mAh g^{-1}) in the first few cycles, underlining that it provides excellent initial performance (no significant kinetic barriers). It decreases exponentially in the 500 cycles, dropping to ~45 mAh g^{-1} by the end. While it performs well initially, its long-term durability in an aqueous environment needs improvement. It is possible that optimizing the curing process (temperature/time) or adding a secondary cross-linker could substantially improve longevity. Indeed, previous studies with modified or co-crosslinked biopolymer binders have achieved hundreds of stable cycles [32,33], so there is room to refine the gluten system.

In summary, for 10% binder long-cycle tests, PVDF provides lower capacity but rock-solid stability, ethyl cellulose provides high capacity but with a steady fading that still retains useful capacity by 500 cycles, and gluten provides high capacity initially but suffers an exponential loss during 500 cycles, indicating the need for further binder optimization. The fact that EC and gluten allowed much higher capacity utilization of LMO initially is encouraging for applications where energy density is paramount, but ensuring long-term stability will be key for these alternatives to truly replace PVDF in commercial systems. It should be noted that in a full cell or practical system, cycle life might be limited by other factors (e.g., the counter electrode or electrolyte); nonetheless, improving binder longevity (perhaps through composite binders or additives) is an important direction for future work.

3.4. Electrode Morphology Studies

Scanning electron microscopy studies were carried out for the electrode that contained 10% gluten. The SEM pictures show how uniformly the binder covers particles and how the microstructure evolves after cycling (Figure 5). The fresh electrode (Figure 5a,b) shows a relatively uniform surface with moderate cracking, and the postmortem electrode after 500 cycles (Figure 5c,d) reveals increased surface fragmentation, deep cracking, and signs of binder degradation and delamination.

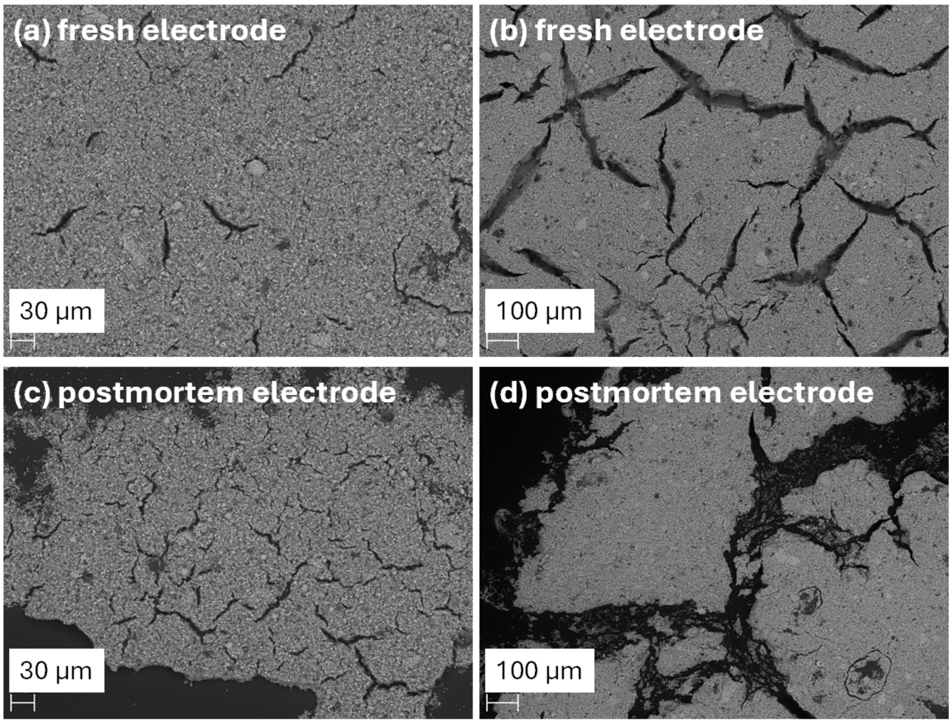

Figure 5. SEM images of LMO electrodes with 10% gluten binder: (**a**,**b**) fresh electrode at two magnifications 30 µm and 100 µm scale and (**c**,**d**) postmortem electrode after 500 cycles.

Elemental analysis by EDS provided postmortem insights into binder and electrode degradation, complementing the morphological observations obtained by SEM. This analysis is particularly valuable when evaluating novel or bio-based binders such as gluten. Since LMO is known to undergo gradual Mn dissolution in aqueous electrolytes—especially during prolonged cycling—chemical changes at the electrode surface can serve as indirect indicators of binder performance. A binder that forms a protective coating around the active material may help limit electrolyte penetration and thereby reduce Mn leaching.

Table 2 summarizes semi-quantitative EDS results averaged over multiple spectra collected from distinct regions of the electrode surface in both fresh and post-cycled LMO electrodes containing 10% gluten binder (with Super P). This data provides a comparative overview and differs from the individual EDS spectra shown in Figure 6, which illustrate local variations. Although the EDS maps and spectra showed heterogeneity, the averaging approach allows for the identification of meaningful comparative trends. After electrochemical cycling, a reduction in Mn signal was observed (from 42 to 34 wt.%), likely indicating Mn dissolution or redistribution. Concurrently, an increase in carbon content (from 24 to 33 wt.%) may reflect binder degradation, Mn loss, and increased exposure of the conductive carbon (Super P). It should be noted that EDS provides only surface-averaged semi-quantitative data; a more rigorous method, such as ICP-OES analysis of the electrolyte solution, would provide more accurate quantification of Mn dissolution. This limitation will be addressed in future work.

Table 2. Averaged EDS results for LMO electrodes with 10% gluten binder before and after 500 cycles. Values represent the mean elemental composition (wt%) from multiple regions across the electrode surface.

Element	Fresh Electrode	Post-Mortem Electrode
Manganese (Mn)	42	34
Carbon (C)	24	33
Sulphur (S)	0.09	0.01
Nitrogen (N)	3.1	2.4

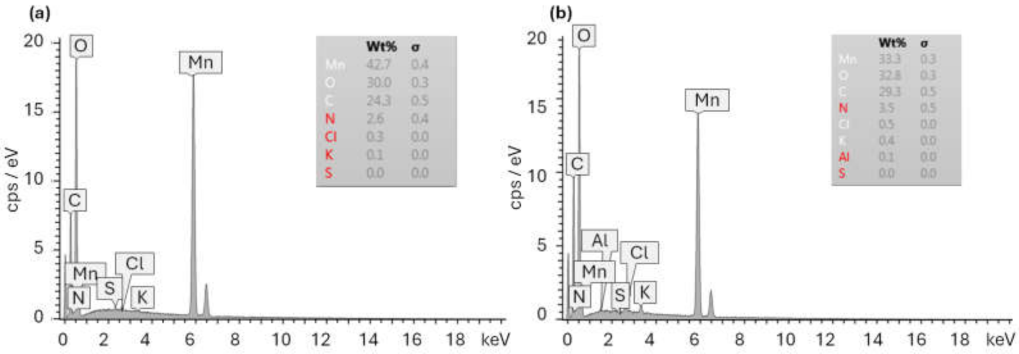

	Wt%	σ
Mn	42.7	0.4
O	30.0	0.3
C	24.3	0.5
N	2.6	0.4
Cl	0.3	0.0
K	0.1	0.0
S	0.0	0.0

	Wt%	σ
Mn	33.3	0.3
O	32.8	0.3
C	29.3	0.5
N	3.5	0.5
Cl	0.5	0.0
K	0.4	0.0
Al	0.1	0.0
S	0.0	0.0

Figure 6. SEM-EDS area-averaged spectra of LMO electrodes with 10% gluten binder (**a**) before and (**b**) after 500 cycles in aqueous electrolyte.

Notably, the sulphur signal—originating from sulphur-containing amino acids in gluten—dropped significantly (from 0.09 to 0.01 wt.%), suggesting considerable binder degradation, particularly through disruption of disulfide cross-links. A decline in nitrogen content (from 3.1 to 2.4 wt.%) was also observed, which may indicate denaturation, leaching, or electrochemical decomposition of the protein matrix. A similar pattern is visible in the area-averaged SEM-EDS spectra shown in Figure 6, supporting these findings.

In areas exhibiting severe degradation, sulphur was no longer detectable in the EDS surface maps. The spatial variability of sulphur and nitrogen signals is consistent with the inherently inhomogeneous distribution of biopolymer binders. These findings underscore the susceptibility of cross-linked gluten to degradation under prolonged aqueous cycling and suggest that further optimization—such as improved chemical cross-linking or protective surface coatings—may be required to enhance long-term binder stability.

4. Discussion

Mechanical and Interfacial Considerations

The performance of electrode binders in lithium-ion batteries is governed not only by their chemical and electrochemical stability, but also by their influence on mechanical cohesion, ionic transport, and electrode morphology. This study compared three types of binders—polyvinylidene fluoride (PVDF), ethyl cellulose, and gluten—each tested at 5% and 10% weight content in the electrode. The results reveal significant differences in initial specific capacity, long-term cycling behaviour, and capacity retention under increasing C-rates. The above results illustrate that binder selection impacts not only environmental sustainability but also cell performance metrics. It is therefore useful to discuss the mechanical and interfacial properties of these binders in the context of electrode function.

PVDF is well-known for its excellent mechanical strength and flexibility, which translates into strong adhesion of active material particles to each other and to the current collector. PVDF's ductile, non-reactive fluoropolymer structure imparts robust cohesion, allowing electrodes to endure volume changes and stresses without cracking or delamination [21]. This partly explains the long cycle life observed with PVDF—it simply does not break apart.

Ethyl cellulose, being a cellulose derivative, provides good adhesive strength as well, though it is somewhat more brittle than PVDF. EC forms a polymer network that adequately binds particles; while it may not be as elastomeric as PVDF, prior studies have shown it can maintain electrode cohesion under repeated cycling [4,21]. One advantage of EC is that it does not swell or dissolve in water, so after drying it remains intact in the aqueous electrolyte, avoiding the extreme swelling that water-soluble binders (like carboxymethyl cellulose or polyacrylic acid) would experience [8]. This helps preserve the electrode structure, though some gradual mechanical degradation (as seen by capacity fade) can still occur, potentially due to minor swelling or softening in the electrolyte over time.

Cross-linked gluten yields a different mechanical profile, as thermally cured gluten forms a flexible, rubbery network. The heating causes the proteins (gliadin and glutenin fractions) to cross-link via mechanisms like disulfide bond formation, which significantly improves film toughness and elasticity [18]. The resulting gluten binder can accommodate strain and maintain contact between particles during cycling, much like PVDF.

In our short-term and rate tests, the gluten-bound electrodes did not show excessive cracking or early capacity loss, indicating decent mechanical resilience (Figure 5). However, the eventual capacity loss by ~500 cycles suggests that the gluten binder might have slowly absorbed water or undergone structural fatigue that PVDF and EC did not. It is worth noting that, unlike PVDF and EC, gluten is a polypeptide that could be more susceptible to chemical degradation (e.g., hydrolysis) over long periods in water, especially if not fully cross-linked. Ensuring a high degree of cross-linking or blending gluten with a secondary polymer (to reinforce it) could mitigate this. The absence of any soluble components from the gluten binder is a positive—once cured, it does not dissolve—so the failure is likely mechanical rather than chemical dissolution.

Interfacial characteristics are also relevant. A good binder should facilitate close contact between the electrolyte and the active particles (for ionic transport) while also ensuring electronic connectivity via the conductive additive network. PVDF, being hydrophobic, can in some cases limit electrolyte wetting at the electrode interface, whereas more polar or hydrophilic binders (like many natural polymers) might allow better electrolyte penetration. Ethyl cellulose is modestly polar (due to $–OC_2H_5$ groups), and gluten is hydrophilic until cross-linked (after which it becomes water-insoluble but still slightly hydroscopic). In our experience, the EC and gluten slurries wetted the substrate and particles well, and the cured coatings did not inhibit electrolyte access. Indeed, the high capacities achieved suggest efficient ionic transport in those electrodes. PVDF electrodes, especially at 10% loading, might have had regions less accessible to the aqueous electrolyte due to PVDF's hydrophobicity and the reduced pore volume (because PVDF can dry to form a film that partly occludes pores). This difference in wetting could partly explain why the 10% PVDF sample underperformed at even moderate rates, whereas the bio-binders allowed better usage of LMO. For future studies, strategies such as EC-alginate blends or mild cross-linking will be considered.

Lastly, it is important to consider the broader implications for solid-boosted FBs. The binder in each booster particle must withstand mechanical abrasion (particles colliding) and continuous contact with flowing electrolyte. From our findings, a binder like PVDF would likely hold particles together but raises sustainability and processing concerns (needing NMP, etc.), whereas ethyl cellulose and gluten could enable a fully green processing (water/alcohol-based). Ethyl cellulose looks particularly promising as it combines high performance with decent stability. Gluten showed that natural materials can work, but their long-term stability in an FB tank is questionable without further improvements. Still, even if gluten required periodic re-curing or replacement, its environmental benignity and cost (being essentially a food byproduct) could be advantageous. One possible mitigation for gluten's degradation could be coatings on the booster particles—for instance, a thin protective coating (like alginate or a shellac) over the gluten-bound particle to seal it from direct water exposure, while still allowing ion transport. These strategies are beyond the scope of the present study but represent promising directions for future research.

5. Conclusions

This study demonstrates that both ethyl cellulose and cross-linked gluten are viable, eco-friendly alternatives to PVDF in aqueous lithium-ion battery electrodes. Replacing PVDF with these natural binders dramatically improves the sustainability of electrode manufacturing: it enables safer processing (no toxic NMP fumes), faster electrode drying, and eliminates the need for costly solvent recovery systems. These advantages make the bio-binders highly attractive for large-format energy storage systems, where environmental regulations and safety requirements can drive up costs. The only processing trade-off is that gluten binders require an extra curing step (heating to 150 °C) to achieve water resistance, but this can be conveniently integrated into the standard drying process and is a one-time treatment. Electrochemically, our comparative tests showed that ethyl cellulose and gluten can replace PVDF without major sacrifices in performance. In fact, at 5% binder loading, both alternatives enabled higher initial capacities (~90–100·mAh g^{-1} at 0.2–1 C) than a traditional 10% PVDF electrode (~40 mAh g^{-1} at 1 C). Ethyl cellulose excelled in initial performance, and even though it exhibited some capacity fade over long cycling, it maintained a useful capacity (>50% of initial) over 500 cycles. Cross-linked gluten delivered comparable initial results and stable medium-term cycling (tens of cycles), though its long-term durability needs improvement as currently implemented. Notably, both ethyl cellulose and gluten binders produce electrodes that are completely free of fluoropolymers and toxic solvents, aligning with the push for greener battery technologies. This means an entire cell can be made without PFAS or hazardous components when using these binders (especially in combination with an aqueous electrolyte), greatly simplifying end-of-life disposal or recycling. Each alternative binder has its strengths. Ethyl cellulose offers a very straightforward transition for industry—it uses a volatile, low-toxicity solvent (alcohol) and requires no special treatment, while delivering reliable mechanical and electrochemical performance close to PVDF. Crosslinked gluten allows an even greener process (water-based, no organic solvents at all) and, after curing, shows surprisingly good mechanical robustness (on par with soft polymers) due to protein network formation. The weaknesses observed—namely, the slightly higher capacity fade for ethyl cellulose and the exponential capacity loss for gluten—are not seen as fundamental barriers but rather as issues that can be addressed with further optimization (for instance, improved cross-linking density for gluten, or binder mixes to stabilize ethyl cellulose). The fact that these binders achieved near-PVDF performance in our tests is a significant outcome, as it underscores that moving away from PVDF is not only feasible but can be performed without compromising cell function in aqueous systems.

In aqueous lithium-ion batteries, the use of ethyl cellulose or gluten as binders allows for the elimination of toxic and environmentally harmful components, complementing the safer water-based electrolyte. In solid-boosted flow batteries, these binders can simplify manufacturing and enhance recyclability, as the absence of fluorinated polymers facilitates material recovery and reduces environmental risks from disposal. This study demonstrates that sustainable binders like ethyl cellulose and cross-linked gluten can enable environmentally friendly energy storage systems without compromising reliability. With further optimization of formulation and long-term stability, biodegradable, PFAS-free binders could be confidently adopted in large-scale battery applications.

Author Contributions: Conceptualization, S.S. and P.P.; funding acquisition, S.S.; methodology, S.S. and P.P.; formal analysis, S.S. and M.P.; investigation, S.S. and M.P.; data curation, S.S. and M.P.; writing—original draft preparation, S.S., P.P. and M.P.; writing—review and editing, S.S., P.P. and M.P. All authors have read and agreed to the published version of the manuscript.

Funding: This research was funded by the Estonian Research Council grant MOBTP1023, by the Estonian Ministry of Education and Research project TK210 and Estonian Research Council project TEM-TA69. This work has also partially emanated from the research of P.P. supported by the European Research Council (Starting Grant, agreement no. 950038).

Data Availability Statement: The data supporting the results of this study are not publicly available at this time but may be obtained from the corresponding author upon reasonable request.

Acknowledgments: The authors gratefully acknowledge Marian Külaviir from the Geology Laboratory at the University of Tartu for conducting analytical and imaging work, and Heli Heinikkala from the Department of Mechanical and Materials Engineering at the University of Turku for carrying out initial exploratory laboratory measurements. During the preparation of this manuscript, the authors used ChatGPT (OpenAI, GPT-4, September 2025 version) for the purposes of language editing and proofreading. The authors have reviewed and edited the output and take full responsibility for the content of this publication.

Conflicts of Interest: The authors declare no conflicts of interest.

Abbreviations

The following abbreviations are used in this manuscript:

PVDF	Polyvinylidene Fluoride
ALIBs	Aqueous Lithium-Ion Batteries
FBs	Flow Batteries
LMO	Lithium Manganese Oxide ($LiMn_2O_4$)
NMP	N-Methyl-2-Pyrrolidone
PFAS	Per- and Polyfluoroalkyl Substances
EC	Ethyl Cellulose
CV	Cyclic Voltammetry
SEM	Scanning Electron Microscopy
EDS	Energy-Dispersive X-ray Spectroscopy

References

1. Moghaddam, M.; Sepp, S.; Wiberg, C.; Bertei, A.; Rucci, A.; Peljo, P. Thermodynamics, Charge Transfer and Practical Considerations of Solid Boosters in Redox Flow Batteries. *Molecules* **2021**, *26*, 2111. [CrossRef]
2. Chen, Z.-Y.; He, Y.; Li, Z.-J.; Gao, L.-Z.; Jiang, Q.; Yu, Z.-L. Synthesis and Electrochemical Performance of Spinel $LiMn_2O_4$-x(SO_4)x Cathode Materials. *Chin. J. Chem.* **2002**, *20*, 194–197. [CrossRef]
3. Chen, Z.-Y.; Gao, L.-Z.; Liu, X.-Q.; Yu, Z.-L. Properties and Structure of Spinel Li-Mn-O-F Compounds for Cathode Materials of Secondary Lithium-Ion Battery. *Chin. J. Chem.* **2001**, *19*, 347–351. [CrossRef]
4. Chen, B.; Zhang, Z.; Xiao, M.; Wang, S.; Huang, S.; Han, D.; Meng, Y. Polymeric Binders Used in Lithium Ion Batteries: Actualities, Strategies and Trends. *ChemElectroChem* **2024**, *11*, e202300651. [CrossRef]
5. Yoon, J.; Lee, J.; Kim, H.; Kim, J.; Jin, H.-J. Polymeric Binder Design for Sustainable Lithium-Ion Battery Chemistry. *Polymers* **2024**, *16*, 254. [CrossRef]
6. Lee, S.; Koo, H.; Kang, H.S.; Oh, K.-H.; Nam, K.W. Advances in Polymer Binder Materials for Lithium-Ion Battery Electrodes and Separators. *Polymers* **2023**, *15*, 4477. [CrossRef]
7. Nastasi, L.; Fiore, S. Environmental Assessment of Lithium-Ion Battery Lifecycle and of Their Use in Commercial Vehicles. *Batteries* **2024**, *10*, 90. [CrossRef]
8. Chen, Z.; Kim, G.-T.; Chao, D.; Loeffler, N.; Copley, M.; Lin, J.; Shen, Z.; Passerini, S. Toward Greener Lithium-Ion Batteries: Aqueous Binder-Based $LiNi_{0.4}Co_{0.2}Mn_{0.4}O_2$ Cathode Material with Superior Electrochemical Performance. *J. Power Sources* **2017**, *372*, 180–187. [CrossRef]
9. Chen, H.; Wang, Z.; Feng, Y.; Cai, S.; Gao, H.; Wei, Z.; Zhao, Y. Cellulose-Based Separators for Lithium Batteries: Source, Preparation and Performance. *Chem. Eng. J.* **2023**, *471*, 144593. [CrossRef]
10. Dobryden, I.; Montanari, C.; Bhattacharjya, D.; Aydin, J.; Ahniyaz, A. Bio-Based Binder Development for Lithium-Ion Batteries. *Materials* **2023**, *16*, 5553. [CrossRef]
11. Kim, M.J.; Lee, C.H.; Jo, M.H.; Jeong, S.K. Electrochemical Decomposition of Poly(Vinylidene Fluoride) Binder for a Graphite Negative Electrode in Lithium-Ion Batteries. *Mater. Sci. Forum* **2017**, *893*, 127–131. [CrossRef]
12. Rolandi, A.C.; de Meatza, I.; Casado, N.; Forsyth, M.; Mecerreyes, D.; Pozo-Gonzalo, C. Unlocking Sustainable Power: Advances in Aqueous Processing and Water-Soluble Binders for NMC Cathodes in High-Voltage Li-Ion Batteries. *RSC Sustain.* **2024**, *2*, 2125–2149. [CrossRef]
13. Huang, X.; You, H.; Yan, X.; Borkiewicz, O.J.; Wiaderek, K.M.; Hui, J.; Hersam, M.C.; Chaudhuri, S.; Rowan, S.J.; Chen, J. Environmentally Sustainable Lithium-Ion Battery Cathode Binders Based on Cellulose Nanocrystals. *J. Mater. Chem. A* **2024**, *12*, 33015–33022. [CrossRef]
14. Park, J.; Kim, J.; Kim, J.; Kim, M.; Song, T.; Paik, U. Sustainable and Cost-Effective Electrode Manufacturing for Advanced Lithium Batteries: The Roll-to-Roll Dry Coating Process. *Chem. Sci.* **2025**, *16*, 6598–6619. [CrossRef]
15. Li, J.; Lu, Y.; Yang, T.; Ge, D.; Wood, D.L.; Li, Z. Water-Based Electrode Manufacturing and Direct Recycling of Lithium-Ion Battery Electrodes—A Green and Sustainable Manufacturing System. *iScience* **2020**, *23*, 101081. [CrossRef] [PubMed]
16. Cholewinski, A.; Si, P.; Uceda, M.; Pope, M.; Zhao, B. Polymer Binders: Characterization and Development toward Aqueous Electrode Fabrication for Sustainability. *Polymers* **2021**, *13*, 631. [CrossRef] [PubMed]
17. Nordqvist, P.; Lawther, M.; Malmström, E.; Khabbaz, F. Adhesive Properties of Wheat Gluten after Enzymatic Hydrolysis or Heat Treatment—A Comparative Study. *Ind. Crops Prod.* **2012**, *38*, 139–145. [CrossRef]
18. Lagrain, B.; Thewissen, B.G.; Brijs, K.; Delcour, J.A. Mechanism of Gliadin–Glutenin Cross-Linking during Hydrothermal Treatment. *Food Chem.* **2008**, *107*, 753–760. [CrossRef]
19. Dong, T.; Mu, P.; Zhang, S.; Zhang, H.; Liu, W.; Cui, G. How Do Polymer Binders Assist Transition Metal Oxide Cathodes to Address the Challenge of High-Voltage Lithium Battery Applications? *Electrochem. Energy Rev.* **2021**, *4*, 545–565. [CrossRef]
20. Liu, G.; Zheng, H.; Song, X.; Battaglia, V.S. Particles and Polymer Binder Interaction: A Controlling Factor in Lithium-Ion Electrode Performance. *J. Electrochem. Soc.* **2011**, *159*, A214. [CrossRef]
21. Yoon, H.; Behera, P.; Lim, S.; Yun, T.G.; Hwang, B.; Cheong, J.Y. Review of the Mechanistic and Structural Assessment of Binders in Electrodes for Lithium-Ion Batteries. *Int. J. Energy Res.* **2024**, *2024*, 8893580. [CrossRef]
22. Machado Pico, P.P.; Colonna, S.; Ronci, F. Low-Cost, Sustainable Hybrid Aqueous Zinc Metal Batteries Using Ethyl Cellulose as a Binder. *Batteries* **2025**, *11*, 189. [CrossRef]
23. Zhou, J.; Wu, S.; Li, Q.; Wu, F. Biologically Insoluble Binder for High-Performance Cathodes in Lithium-Ion Batteries. *Adv. Energy Mater.* **2025**, *15*, 2406032. [CrossRef]
24. Wang, R.; Feng, L.; Yang, W.; Zhang, Y.; Zhang, Y.; Bai, W.; Liu, B.; Zhang, W.; Chuan, Y.; Zheng, Z.; et al. Effect of Different Binders on the Electrochemical Performance of Metal Oxide Anode for Lithium-Ion Batteries. *Nanoscale Res. Lett.* **2017**, *12*, 575. [CrossRef] [PubMed]
25. Qin, T.; Yang, H.; Li, Q.; Yu, X.; Li, H. Design of Functional Binders for High-Specific-Energy Lithium-Ion Batteries: From Molecular Structure to Electrode Properties. *Ind. Chem. Mater.* **2024**, *2*, 191–225. [CrossRef]

26. Tian, Y.; Xie, J.; Tian, M.; Luo, X.; Wang, L.; Zhou, S.; Feng, Y.; Hu, L. Advanced Cathode Binders for Lithium-Ion Batteries: Molecular Design and Performance Enhancement. *Chem. Eng. J. Adv.* **2025**, *24*, 100838. [CrossRef]
27. Srivastava, M.; M. R., A.K.; Zaghib, K. Binders for Li-Ion Battery Technologies and Beyond: A Comprehensive Review. *Batteries* **2024**, *10*, 268. [CrossRef]
28. Kuenzel, M.; Choi, H.; Wu, F.; Kazzazi, A.; Axmann, P.; Wohlfahrt-Mehrens, M.; Bresser, D.; Passerini, S. Co-Crosslinked Water-Soluble Biopolymers as a Binder for High-Voltage $LiNi_{0.5}Mn_{1.5}O_4$ | Graphite Lithium-Ion Full Cells. *ChemSusChem* **2020**, *13*, 2650–2660. [CrossRef]
29. Savvidou, E.K.; Rensmo, A.; Benskin, J.P.; Schellenberger, S.; Hu, X.; Weil, M.; Cousins, I.T. PFAS-Free Energy Storage: Investigating Alternatives for Lithium-Ion Batteries. *Environ. Sci. Technol.* **2024**, *58*, 21908–21917. [CrossRef]
30. Bigoni, F.; Giorgio, F.D.; Soavi, F.; Arbizzani, C. Sodium Alginate: A Water-Processable Binder in High-Voltage Cathode Formulations. *J. Electrochem. Soc.* **2016**, *164*, A6171. [CrossRef]
31. Versaci, D.; Nasi, R.; Zubair, U.; Amici, J.; Sgroi, M.; Dumitrescu, M.A.; Francia, C.; Bodoardo, S.; Penazzi, N. New Eco-Friendly Low-Cost Binders for Li-Ion Anodes. *J. Solid State Electrochem.* **2017**, *21*, 3429–3435. [CrossRef]
32. Gu, Y.; Yang, S.; Zhu, G.; Yuan, Y.; Qu, Q.; Wang, Y.; Zheng, H. The Effects of Cross-Linking Cations on the Electrochemical Behavior of Silicon Anodes with Alginate Binder. *Electrochim. Acta* **2018**, *269*, 405–414. [CrossRef]
33. Lee, D.; Park, H.; Goliaszewski, A.; Byeun, Y.; Song, T.; Paik, U. In Situ Cross-Linked Carboxymethyl Cellulose-Polyethylene Glycol Binder for Improving the Long-Term Cycle Life of Silicon Anodes in Li Ion Batteries. *Ind. Eng. Chem. Res.* **2019**, *58*, 8123–8130. [CrossRef]